International Journal of Thermophysics (2020) 41:78
https://doi.org/10.1007/s10765-020-02662-3

INVITED REVIEW

Photopyroelectric Spectroscopy of Pure Fluids and Liquid Mixtures: Foundations and State-of-the-Art Applications

J. A. Balderas-López[1] · A. Mandelis[2]

Received: 17 March 2020 / Accepted: 28 March 2020 / Published online: 4 April 2020

Abstract
Since the mathematical foundations of photothermal effects in condensed phase materials were established in the middle 1970s, new photothermal methodologies have emerged based on the detection of heat generated from the absorption and non-radiative conversion of modulated radiation. Among them, photopyroelectric techniques have become very popular and widely used for a variety of studies ranging from calorimetry (photothermal calorimetry), phase transitions and the measurement of thermophysical (thermal diffusivity, effusivity and conductivity) and optical properties (photopyroelectric spectroscopy). More recently photopyroelectric detection has been used for the direct quantification of the optical absorption coefficient of condensed phase materials and has demonstrated its potential for quantitative analysis. In this work, a survey of various applications of photopyroelectric detection for the analysis of fluids and liquid mixtures is presented with special focus on theoretical and experimental progress in quantitative analytical measurements as new developments in this field.

Keywords Photopyroelectric spectroscopy · Pure fluids and mixtures · Qualitative and quantitative analysis

1 Introduction and Background

The discovery of pyroelectricity dates back to the time of the Ancient Greeks, when Theophrastus, in 314 B.C. discovered this effect in tourmaline crystals [1, 2]. Originally used for the detection of radiation, through the heating caused in the sensor

✉ J. A. Balderas-López
abrahambalderas@hotmail.com

[1] Basic Science Department, Instituto Politécnico Nacional-UPIBI, Avenida Acueducto S/N, col. Barrio la Laguna, Ticomán, Del. Gustavo A. Madero, 07340 México City, México

[2] Center for Advanced Diffusion-Wave and Photoacoustic Technologies (CADIPT), Department of Mechanical and Industrial Engineering, University of Toronto, 5 King's College Road, Toronto, ON M5S 3G8, Canada

by the absorption of photons [3], developments in materials science and technology have allowed the synthesis of new and much improved pyroelectric sensors and this has made possible their use in a great variety of scientific and technological fields. In the past 35 years, pyroelectric sensors have found applications as radiation sensors, in gas sensing, for the construction of thermal images, and as temperature sensors, among other uses [4–7]. A unique feature of pyroelectric sensors is their sensitive response to time-dependent heat sources, which makes them ideal for the detection of thermal waves, that is, harmonic temperature fluctuations stemming from the absorption of modulated radiation in a material.

Modulated pyroelectric detection of photothermal generation from pulsed and harmonic optical sources in solids and thin films was introduced independently by Mandelis [8] and Coufal [9], respectively. The term "photopyroelectric" was coined, and the mathematical basis for the frequency-domain signal interpretation presented, by Mandelis in 1984 [8]. The first detailed theoretical analysis of the PPE signal detected by a pyroelectric sensor, with the interrogated material in intimate contact with the sensor, was subsequently developed by Mandelis and Zver in 1985 [10]. In these two works the authors discussed sample configuration, geometric, thermophysical and optical property measurement conditions under which the PPE signal can be expressed in terms of simple expressions and can be directly related to those properties of an investigated sample, notably its optical absorption coefficient, thereby giving rise to photopyroelectric spectroscopy (PPES) which soon after was applied to extracting qualitative absorption spectra of solids [11]. Later on, Chirtoc and Mihâilescu [12] presented a systematic classification of the photopyroelectric (PPE) signals that included sensor surface reflectivity, to support quantitative thermal and optical studies of condensed matter.

One of the advantages of PPE techniques over other related photothermal methods is the ability to use several experimental control variables and thus obtain several physical properties of a sample under study. One of the first applications of these techniques was the qualitative spectroscopic (optical absorption coefficient) study of condensed phase materials using the wavelength of the exciting radiation as control parameter [11, 13]. Researchers soon realized the wider potential of PPE detection and the range of applications was extended to many other fields of science and engineering which are currently used in calorimetric studies, for measuring specific heats [14], phase transitions in a variety of materials [15–17], and for thermophysical measurements of thermal diffusivity, thermal conductivity and thermal effusivity, using modulation frequency as a control variable [18–21]. The development of the so-called thermal wave resonator cavity (TWRC) by Shen and Mandelis in 1995 [22], in which the sample thickness is used as a control variable, opened another area of possibilities for high-precision thermophysical characterization of gases and liquids [23–27].

To simplify the TWRC analysis, mathematical models have involved purely thermal responses of fluid samples without signal contributions from their optical properties. The conditions for this simplification which leads to simple and highly precise thermophysical measurements are generally satisfied by inserting a very thin opaque layer between the light source and the liquid sample. However, the flexibility of letting light go through the sample allows for the development of PPE techniques for

the direct measurement of optical absorption coefficients of liquid samples, as was theoretically predicted by Mandelis and Zver [10] and by Chirtoc and Mihâilescu [12], and was implemented in practice by Balderas-López et al. [28–30]. The spectroscopy extension of the PPE technique has been used for optical absorption coefficient and quantum yield measurements in optical solids [31–33], and has shown advantages over conventional spectroscopic methods. For instance, in conventional quantitative spectroscopy, absorbance, a non-dimensional parameter, is simply defined as the negative logarithm of the ratio between the light intensity passing through a fixed sample thickness and the intensity incident on the sample. This non-dimensional number, however, takes on quantitative meaning only in the context of the Beer–Lambert model for light absorption because only under this assumption, absorbance and optical absorption coefficient are proportional. When using conventional spectroscopy for quantification purposes a calibration curve is required. This calibration curve validates the linear relation between absorbance and optical absorption coefficient and thus with the absorbing chromophore concentration in a fluid sample mixture. In practice, the measurement dynamic range depends on the spectroscopic technique. Conventional spectroscopy, usually in the transmission mode, is convenient only for small concentrations of the absorbing chromophore in the mixture. Light reflections at the interface of the sample and the container wall present a complication due to light losses for which compensation through a reference medium (usually the solvent in the mixture) is required. The measurement of a reference sample to obtain a calibration curve is especially inconvenient when dealing with optical property measurements of pure fluids or fluids in the form of diluted mixtures, such as vegetable oils. These inconveniences are not a problem when using PPE techniques at fixed modulation frequency and taking sample thickness as the control parameter.

The purpose of this review is to provide examples of measurements of thermal diffusivity and optical absorption coefficient of liquids and demonstrate the use of these properties as convenient parameters for qualitative and quantitative thermophysical analysis of fluids.

2 General Photopyroelectric Theory

Mathematical models of frequency-domain photopyroelectric detection typically used in quantitative analysis follow the configuration described in Fig. 1. The experimental setup consists of monochromatic radiation modulated at frequency f, which travels through a transparent medium $\boldsymbol{v}$ to eventually reach media $\boldsymbol{s}$, $\boldsymbol{w}$ and $\boldsymbol{p}$, ending at a semi-infinite and transparent layer $\boldsymbol{g}$. Radiation is assumed to be absorbed across those materials following the Beer–Lambert law with optical absorption coefficients β_s, β_w and β_p, respectively. The optical properties of medium $\boldsymbol{g}$ are not relevant in this case since strong optical absorption will be assumed for the pyroelectric material. In this figure $\boldsymbol{s}$ represents the fluid under study and $\boldsymbol{p}$ the pyroelectric sensor. $\boldsymbol{w}$ represents an optional pyroelectric protective layer which does not have any influence on the main results as will be shown later. If no internal optical reflections and infrared radiation at the various interfaces are present (a more complete model is

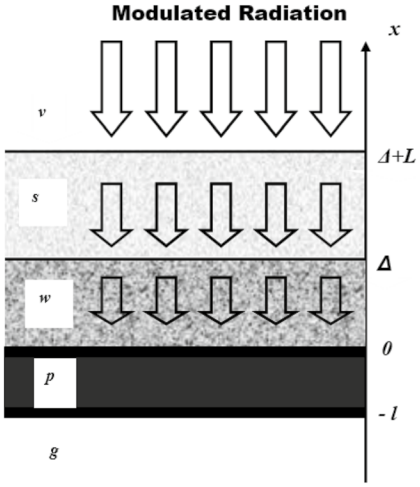

Fig. 1 Schematic representation of the one-dimensional 3-layered model. Media ***s***, ***p*** and ***w*** are assumed to absorb light according the Beer–Lambert model

described by Mandelis and da Silva [34]), the corresponding set of one-dimensional differential heat diffusion equations is

$$\begin{aligned}
\frac{\partial^2 T_v}{\partial x^2} - \frac{1}{\alpha_v}\frac{\partial T_v}{\partial t} &= 0 && L+\Delta \le x \\
\frac{\partial^2 T_s}{\partial x^2} - \frac{1}{\alpha_s}\frac{\partial T_s}{\partial t} &= -\frac{\beta_s I_0}{k_s} e^{\beta_s (x-L-\Delta)} e^{i\omega t} && \Delta \le x < L+\Delta \\
\frac{\partial^2 T_w}{\partial x^2} - \frac{1}{\alpha_w}\frac{\partial T_w}{\partial t} &= -\frac{\beta_w I_0}{k_w} e^{-\beta_s L} e^{\beta_w (x-\Delta)} e^{i\omega t} && 0 \le x < \Delta \\
\frac{\partial^2 T_p}{\partial x^2} - \frac{1}{\alpha_p}\frac{\partial T_p}{\partial t} &= -\frac{\beta_p I_0}{k_p} e^{-\beta_s L} e^{-\beta_w \Delta} e^{\beta_p x} e^{i\omega t} && -l \le x < 0 \\
\frac{\partial^2 T_g}{\partial x^2} - \frac{1}{\alpha_g}\frac{\partial T_g}{\partial t} &= 0 && -\infty < x \le -l
\end{aligned} \quad , \tag{1}$$

where T_j, $j = v,s,w,p,g$ refers to the temperature profile inside medium j with k_j and α_j being its thermal conductivity and diffusivity, respectively. The PPE signal is the average thermal-wave field distribution inside medium ***p***. The set of equations (1) is coupled through interfacial boundary conditions of temperature and heat flux continuity. Solving the set of differential equations (1), assuming a fully opaque pyroelectric sensor ($\beta_p \to \infty$), yields the PPE voltage developed across the detector [29]:

$$
\begin{aligned}
V_p = {} & \frac{KI_0}{lk_p\sigma_p^2 D}\left\{(1+b_{gp})e^{\sigma_p l} - (1-b_{gp})e^{-\sigma_p l} - 2b_{gp}\right\} \\
& * \left(e^{-\beta_s L}e^{-\beta_w \Delta}\left\{ \frac{b_{pw}r_w}{(1-r_w^2)}\left[(1+b_{vs})(1+b_{ws})(1+r_w)e^{\sigma_s L}e^{\sigma_w \Delta} - (1-b_{vs})(1-b_{ws})(1+r_w)e^{-\sigma_s L}e^{\sigma_w \Delta}\right.\right.\right. \\
& \left. + (1+b_{vs})(1-b_{ws})(1-r_w)e^{\sigma_s L}e^{-\sigma_w \Delta} - (1-b_{vs})(1+b_{ws})(1-r_w)e^{-\sigma_s L}e^{-\sigma_w \Delta}\right] \\
& + b_{pw}\left[(1+b_{vs})(1+b_{ws})e^{\sigma_s L}e^{\sigma_w \Delta} - (1-b_{vs})(1-b_{ws})e^{-\sigma_s L}e^{\sigma_w \Delta} - (1+b_{vs})(1-b_{ws})e^{\sigma_s L}e^{-\sigma_w \Delta}\right. \\
& \left. + (1-b_{vs})(1+b_{ws})e^{-\sigma_s L}e^{-\sigma_w \Delta}\right] \\
& + 2e^{-\beta_s L}\left[\frac{b_{pw}r_w}{(1-r_w^2)}\left[(1-b_{vs})(1-b_{ws}r_w)e^{-\sigma_s L} - (1+b_{vs})(1+b_{ws}r_w)e^{\sigma_s L}\right]\right. \\
& \left.\left. + \frac{b_{ps}r_s}{(1-r_s^2)}\left[(1+b_{vs})(1+r_s)e^{\sigma_s L} - (1-b_{vs})(1-r_s)e^{-\sigma_s L}\right]\right] - \frac{4b_{ps}r_s(r_s+b_{vs})}{(1-r_s^2)}\right),
\end{aligned}
\tag{2}
$$

where

$$
\begin{aligned}
D = {} & M\left[(1-b_{gp})(1-b_{pw})e^{-\sigma_p l}e^{\sigma_w \Delta} + (1+b_{gp})(1+b_{pw})e^{\sigma_p l}e^{\sigma_w \Delta}\right] \\
& + N\left[(1-b_{gp})(1+b_{pw})e^{-\sigma_p l}e^{-\sigma_w \Delta} + (1+b_{gp})(1-b_{pw})e^{\sigma_p l}e^{-\sigma_w \Delta}\right],
\end{aligned}
$$

$$
\begin{aligned}
M &= (1+b_{vs})(1+b_{ps})e^{\sigma_s L} - (1-b_{vs})(1-b_{ps})e^{-\sigma_s L}, \\
N &= (1+b_{vs})(1-b_{ps})e^{\sigma_s L} - (1-b_{vs})(1+b_{ps})e^{-\sigma_s L}.
\end{aligned}
$$

Here, $r_j = \beta_j/\sigma_j$, $\sigma_j = (1+i)(\pi f/\alpha_j)^{1/2}$, $j = p,s,w$ and $b_{jk} = e_j/e_k$ is the ratio of thermal effusivities of media j and k. K in this equation involves physical properties, including the transfer function of the pyroelectric material, and some other constants that are not relevant to the measured fluid properties.

Two experimental limits are especially useful and involve the sample fluid in the thermally thick limit.

3 Weakly Absorbing Sample in the Thermally Thick Limit

If the thermally thick limit is assumed for medium s in Eq. 2 (i.e., $|\sigma_s L| >> 1$ such that $\exp(-\sigma_s L) \sim 0$ and $\exp(\sigma_s L) \to \infty$), and at the same time the last term $\frac{4b_{ps}r_s(r_s+b_{vs})}{(1-r_s^2)}$ is neglected, a simplification justified in the limit of weakly absorbing samples (this assumption is well justified for liquids since, in this case, b_{ij} is of the order of one and taking for instance a water solution with $\beta_s = 10$ cm^{-1}, the amplitude of r_s is $|r_s| \sim 0.21$, at $f = 1$ Hz. In this way the expression under consideration is very small as compared to the exponential behavior assumed for this case, $\exp(\sigma_s L) \to \infty$), Eq. 3 simplifies to

$$V_p = \frac{KI_0}{lk_p\sigma_p^2 D_{TG}}\left\{(1+b_{gp})e^{\sigma_p l} - (1-b_{gp})e^{-\sigma_p l} - 2b_{gp}\right\}$$
$$* e^{-\beta_s L}\left(e^{-\beta_w \Delta}\left\{\frac{b_{pw}r_w}{(1-r_w^2)}\left[(1+b_{ws})(1+r_w)e^{\sigma_w\Delta} + (1-b_{ws})(1-r_w)e^{-\sigma_w\Delta}\right]\right.\right.$$
$$\left. + b_{pw}\left[(1+b_{ws})e^{\sigma_w\Delta} - (1-b_{ws})e^{-\sigma_w\Delta}\right]\right\}$$
$$\left. + 2\left[\frac{b_{ps}r_s}{(1+r)} - \frac{b_{pw}r_w}{(1-r_w^2)}(1+b_{ws}r_w)\right]\right), \tag{3}$$

where

$$D_{TG} = (1+b_{ps})(1-b_{gp})(1-b_{pw})e^{-\sigma_p l}e^{\sigma_w\Delta} + (1-b_{ps})(1-b_{gp})(1+b_{pw})e^{-\sigma_p l}e^{-\sigma_w\Delta}$$
$$+ (1+b_{ps})(1+b_{gp})(1+b_{pw})e^{\sigma_p l}e^{\sigma_w\Delta} + (1-b_{ps})(1+b_{gp})(1-b_{pw})e^{\sigma_p l}e^{-\sigma_w\Delta}.$$

If the PPE signal is considered to be solely a function of the sample thickness (L), Eq. 3 can be written in the very simple form [12, 29]:

$$V_p(L) = Ce^{-\beta_s L}, \tag{4}$$

where

$$C = \frac{KI_0}{lk_p\sigma_p^2 D_{TG}}\left\{(1+b_{gp})e^{\sigma_p l} - (1-b_{gp})e^{-\sigma_p l} - 2b_{gp}\right\}$$
$$\left(e^{-\beta_w \Delta}\left\{\frac{b_{pw}r_w}{(1-r_w^2)}\left[(1+b_{ws})(1+r_w)e^{\sigma_w\Delta} + (1-b_{ws})(1-r_w)e^{-\sigma_w\Delta}\right]\right.\right.$$
$$\left. + b_{pw}\left[(1+b_{ws})e^{\sigma_w\Delta} - (1-b_{ws})e^{-\sigma_w\Delta}\right]\right\}$$
$$\left. + 2\left[\frac{b_{ps}r_s}{(1+r)} - \frac{b_{pw}r_w}{(1-r_w^2)}(1+b_{ws}r_w)\right]\right)$$

is a complex expression independent of sample thickness. If the PPE setup is such that the group of terms $\frac{b_{ps}r_s}{(1+r_s)}$ can be neglected in the expression for C, then this expression becomes also independent of the sample optical absorption coefficient. Under this limiting condition, Eq. 4 can be used to obtain qualitative absorption spectra. The experimental procedure for PPE measurements in this case consists of recording the signal as a function of optical wavelength, keeping both modulation frequency and sample thickness constant.

Equation 4 shows that the amplitude of the PPE signal is a simple function of sample thickness, decaying exponentially with increasing thickness while, at the same time, the phase remains constant. This allows the direct measurement of the optical absorption coefficient of a fluid without the requirement of a calibration curve since the constancy of the phase can be taken as an experimental criterion for validation of the analytical procedure. This analytical procedure consists in plotting the amplitude (in semi-log scale) and phase of the PPE signal as a function of sample thickness at controlled increments and fitting the PPE amplitude to a linear model in the thickness range (if any)

where the PPE phase remains approximately constant. According to Eq. 4 the slope of the linear fit yields directly the sample optical absorption coefficient at the wavelength used for the analysis. This methodology can be applied to the direct measurement of the optical absorption coefficient of pure liquids as well as those consisting of dissolved absorbing solutes in liquid mixtures.

For an optically absorbing solute in a liquid mixture, the absorption coefficient at a given excitation wavelength, $\boldsymbol{\beta_s(\lambda,c)}$, is defined as $\boldsymbol{\beta_s(\lambda,c)=\varepsilon(\lambda)c}$, where $\boldsymbol{\varepsilon(\lambda)}$ is the solute absorptivity and $\boldsymbol{c}$ its concentration. The absorptivity is independent of the concentration and is only a function of the absorbing solute and possibly the solvent in which it is diluted. In this case PPE detection can be used for quantitative analysis. The analytical procedure involves measuring the optical absorption coefficient of the mixture and if the corresponding absorptivity is known, the unknown concentration can be obtained as $\boldsymbol{c=\beta_s(\lambda,c)/\varepsilon(\lambda)}$. If the absorptivity is unknown, the quantitative procedure will require prior measurement of the optical absorption coefficient for a mixture of known concentration—a standard procedure—in order to extract this optical property.

For a complex mixture of n absorbing solutes, the optical absorption coefficient at a given wavelength is defined as $\boldsymbol{\beta_s(\lambda,c_1,c_2,\ldots\ c_n)=\varepsilon_1(\lambda)c_1+\varepsilon_2(\lambda)c_2+\cdots\varepsilon_n(\lambda)c_n.}$ The quantitative analysis will require measurements of the optical absorption coefficient of the mixture at n convenient wavelengths (this may require prior calibration measurement of the individual mixture components of known concentrations—standards—so as to extract the individual absorptivities).

Some advantages of PPES over conventional spectroscopies are its much higher dynamic range (this is characteristic of the optical-to-thermal energy conversion origin of the PPE signal which appears only if there is a non-zero absorption in an otherwise zero signal background) and the absence of requirement of a reference sample or calibration curve as described above. These advantages are especially relevant when dealing with the quantification of optically absorbing solutes in multi-component mixtures, calibration curves for which are hard to establish.

4 Strongly Absorbing Sample in the Thermally Thick Limit

On the other extreme, for a thermally thick sample in the high (surface) optical absorption coefficient limit (theoretically $\beta_s \to \infty$, then $\exp(-\beta_s L) \approx 0$ and $r_s \to \infty$), the following simplifications apply:

$$\lim_{r_s\to\infty} \frac{r_s^2}{1-r_s^2} = -1,\ \lim_{r_s\to\infty} \frac{r_s}{1-r_s^2} = 0$$

and Eq. 2 reduces to

$$V_p = \frac{KI_0 4 b_{pv}}{l k_p \sigma_p^2 (1+b_{vs}) D_{TG}} \left\{(1+b_{gp})e^{\sigma_p l} - (1-b_{gp})e^{-\sigma_p l} - 2b_{gp}\right\} e^{-\sigma_s L}. \quad (5)$$

Under this condition the light beam is absorbed along a short distance inside the sample and, contrary to the previous limiting case, the sample optical properties do

not explicitly appear in the equation; only thermal properties can be measured. This approximation is equivalent to the surface absorption model, previously reported by Balderas-López and Mandelis [35], which has been successfully used for the measurement of the thermal diffusivity of two layered systems in the frequency domain.

Considering again the sample thickness L as the only variable, this equation can be written:

$$V_p(L) = He^{-\sigma_s L} \tag{6}$$

as [28, 29], where

$$H = \frac{KI_0 4b_{pv}}{lk_p\sigma_p^2(1+b_{vs})D_{TG}}\left\{(1+b_{gp})e^{\sigma_p l} - (1-b_{gp})e^{-\sigma_p l} - 2b_{gp}\right\}$$

is a complex expression and, like C in Eq. 4, is independent of the thickness, L. Equation 6 shows that both, PPE amplitude (in semi-log scale) and phase have linear behavior as functions of the sample thickness under these conditions. This phase behavior makes the difference between this limiting case and the previous one, for weakly absorbing fluids, where the phase was shown to be a constant.

The analytical treatment of Eq. 6 will yield two very similar slope M values, which result from linear best fits of the PPE amplitude (in semi-log scale) and phase. Two independent thermal diffusivity values can thus be obtained as $\alpha_s = (\pi/M^2)f$.

This methodology can be applied to general liquids just by adding an extra opaque layer on top of the liquid sample. It can be shown that the theoretical model still applies under these conditions, as long as the only variable is the sample thickness L. High-precision measurements of thermal diffusivity of pure fluids and their mixtures can be obtained with this PPE modality and these values can be correlated with the fluid molecular structure or its composition (e.g., for liquid mixtures) [36, 37].

5 Analytical PPEs Experimental Configurations

Figure 2a, b shows, respectively, a schematic cross section and the picture of a typical PPE setup for thermal diffusivity measurements for fluids. The corresponding PPE setup for optical absorption coefficient measurements just involves an optical window instead of the thin opaque lamella (Fig. 2a), allowing light to pass through the liquid sample [24–27]. They consist of a monochromatic light source (diode lasers in this case, but a broadband light source coupled to a monochromator can also be considered for the case of optical property measurements), modulated in intensity at fixed modulation frequency (1 Hz for the results shown in this work). The pyroelectric sensor may be one of many commercially available transducers (PVDF polymer films, $LiTaO_3$, PZT, etc.). The state-of-the-art in PZT sensors involves built-in electrodes that consist of conducting metallic coatings on one sensor surface and a thin metallic plate on the other. This metallic electrode can also act as a strong surface absorber and protective layer.

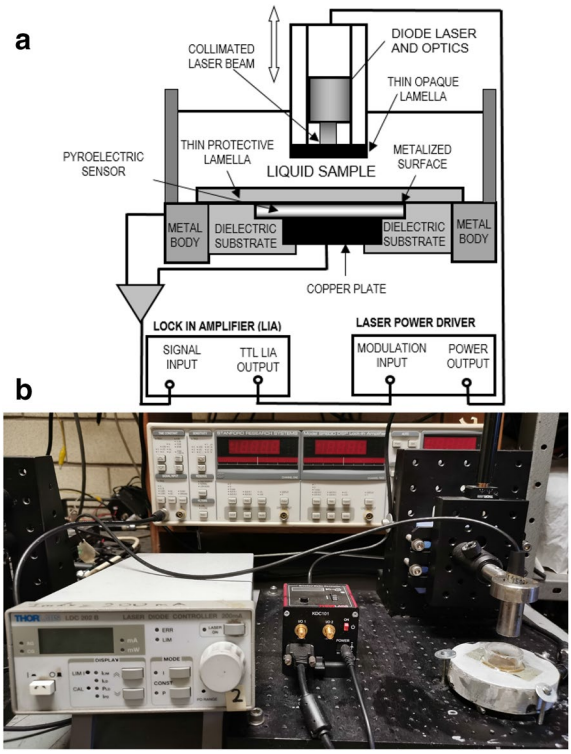

Fig. 2 (a) Schematic cross section of the photopyroelectric setup for thermal diffusivity measurements of fluids. (b) Photograph of the corresponding experimental setup

6 Experimental Results and Discussion

The simplicity and versatility of the photopyroelectric techniques described above allows for the possibility of diverse studies concerning fluids. In what follows, some of these possible applications are described along with some currently ongoing studies.

6.1 Optical Absorption Coefficient Measurements of Pure Fluids

As described in theoretical section, one of the main applications of PPES using the fluid measurement setup described in this work is for optical absorption coefficient measurements of pure liquids. The traditional way of measuring this optical property for pure liquids using conventional spectroscopy resembles the PPE methodology described in this work in the sense that it involves different sample thicknesses (three or more) [38, 39]. A set of sample containers with known light path lengths is required to measure the attenuation of the light as a function of the thickness of the sample. However, it could be problematic to determine the optimum thicknesses by following the Beer–Lambert law without significant interference from internal light reflections. Thermal lens spectroscopy has been used for the measurement of this

optical property for pure liquids, however, it has important limitations due mainly to the complexity of the experimental setup and because it is limited to very weakly absorbing substances [40].

As an example of measuring the optical absorption coefficient of pure liquids using PPES, a near-infrared application is described here that can be extended into any desired spectral range. Figure 3 shows the PPE signal for distilled water at 1310 nm as a function of sample thickness. This plot indicates the sample thickness range within which the PPE phase remains approximately constant (Fig. 3a) and therefore, according to the theoretical model, Eq. 4 applies. The range for analysis was determined by best fitting a straight line from the rightmost experimental point across the group of adjacent flat (horizontal) data points. The corresponding linear fit used for extracting the optical absorption coefficient of distilled water at this wavelength is shown in Fig. 3b. Figure 4 shows the corresponding result for distilled water at a wavelength of 1550 nm. Table 1 summarizes the optical absorption coefficients for this and other pure fluids at four different wavelengths in the near-infrared region. Irving and Pollack [41] collected optical absorption coefficient values for water reported by various authors. In particular, for distilled water they reported the values of 0.067 cm^{-1}, 0.46 cm^{-1}, 1.08 cm^{-1} and 9.6 cm^{-1} at 900 nm, 970 nm, 1310 nm and 1550 nm, respectively. These values are in good agreement with the PPE values reported in this work (Table 1) considering the difference in experimental setups, light sources in particular.

It is interesting to explore the manner in which optical properties behave as function of liquid molecular structure. Linear alcohols are suitable samples for this purpose. Optical absorption coefficients at 1550 nm were measured for a series of linear alcohols, from methanol to 1-decanol (Table 2, column 1). Table 2, column 2 summarizes the optical absorption values obtained at this wavelength. Figure 5 shows

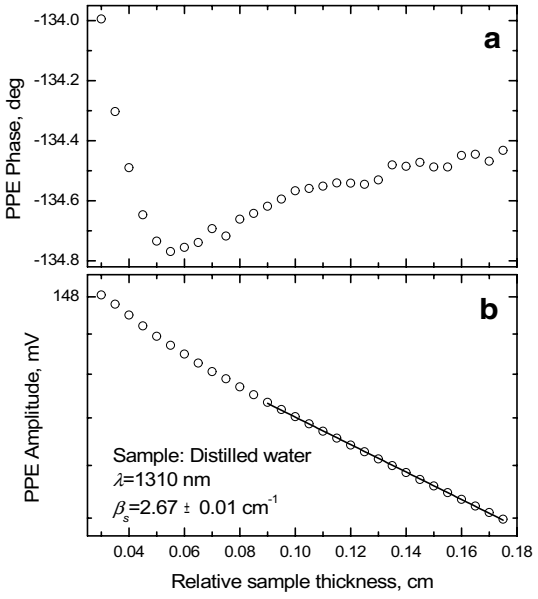

Fig. 3 Photopyroelectric (PPE) signal phase (a) and amplitude (b) of distilled water at 1310 nm as a function of sample thickness. The solid line in (b) is the linear best fit used for extracting the liquid's optical absorption coefficient at this wavelength

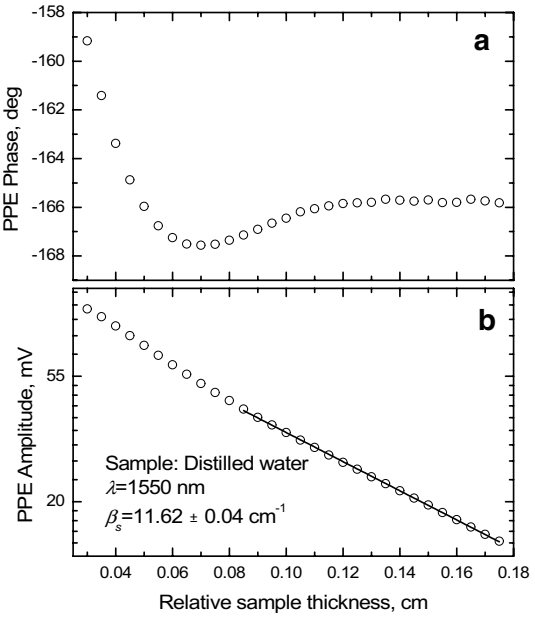

Fig. 4 PPE signal phase (a) and amplitude (b) of distilled water at 1550 nm as a function of sample thickness. The solid line in (b) is the linear best fit used for extracting the liquid's optical absorption coefficient at this wavelength

Table 1 Optical absorption coefficients of some pure liquids in the near-infrared region, measured by means of the photopyroelectric technique [28, 29]

Pure substance	Optical absorption coefficient β (cm^{-1})			
	904 nm	980 nm	1310 nm	1550 nm
Glycerol	0.163 ± 0.001	0.405 ± 0.004	0.893 ± 0.005	11.51 ± 0.03
Distilled water	0.134 ± 0.003	0.695 ± 0.003	2.67 ± 0.010	11.62 ± 0.04
Methanol	0.125 ± 0.005	0.317 ± 0.015	0.686 ± 0.005	9.28 ± 0.03
Ethanol	0.186 ± 0.002	0.298 ± 0.011	0.725 ± 0.003	6.06 ± 0.02

the behavior of this optical property as a function of the sample molar weight. It is interesting to note that the values of this optical property decrease with the size of the molecule and it can be speculated (this requires further close study, of course) that this behavior is related to the molecular structure, the size relation between the OH group and the rest of the molecule could play a main role in this case.

6.2 Optical Absorption Coefficient and Quantitative Analysis for Liquid Mixtures

The PPE methodology has also been proven useful for quantification of liquid–liquid mixtures. Let us consider a liquid mixture consisting of n chemically pure liquids at volumetric fractions of v_i/V, $i=1\ldots n$, where v_i corresponds to the volume of the pure fluid species (i) in the mixture and V is the total volume. The experimental

Table 2 Optical absorption coefficients at 1550 nm, for a series of linear alcohols, measured by means of the photopyroelectric technique [28, 29]

Linear alcohol	β (cm^{-1}) at 1550 nm
Methanol	9.28 ± 0.03
Ethanol	6.06 ± 0.02
1-Propanol	4.9 ± 0.02
1-Butanol	4.18 ± 0.02
1-Pentanol	3.65 ± 0.01
1-Hexanol	3.21 ± 0.01
1-Heptanol	2.9 ± 0.01
1-Octanol	2.74 ± 0.01
1-Nonanol	2.63 ± 0.01
1-Decanol	2.48 ± 0.01

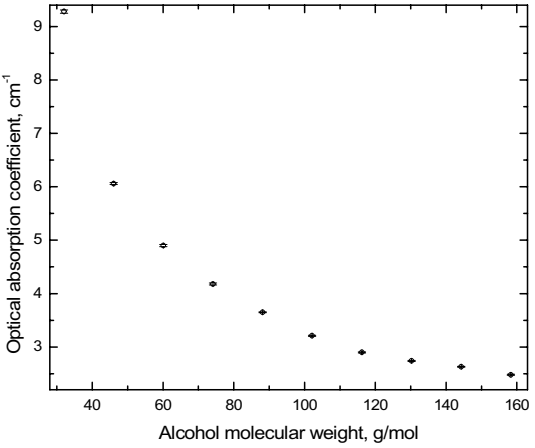

Fig. 5 Optical absorption coefficients at 1550 nm, as a function of molecular weight for linear alcohols

procedure for obtaining these volumetric fractions involves measuring the optical absorption coefficients of the mixture, $\beta(\lambda_j)$, at n conveniently chosen wavelengths λ_j, $j=1\ldots n$, and those, $\beta_i(\lambda_j)$, of each pure fluid component (i), if the latter are unknown. The analytical procedure consists of solving a system of n linear equations:

$$\begin{aligned}
&\alpha_1\beta_1(\lambda_1)+\alpha_2\beta_2(\lambda_1)+\alpha_3\beta_3(\lambda_1)+\cdots+\alpha_n\beta_n(\lambda_1)=\beta(\lambda_1)\\
&\alpha_1\beta_1(\lambda_2)+\alpha_2\beta_2(\lambda_2)+\alpha_3\beta_3(\lambda_2)+\cdots+\alpha_n\beta_n(\lambda_2)=\beta(\lambda_2)\\
&\qquad\qquad\qquad\qquad\qquad\qquad\qquad\qquad\qquad\cdots\\
&\alpha_1\beta_1(\lambda_n)+\alpha_2\beta_2(\lambda_n)+\alpha_3\beta_3(\lambda_n)+\cdots+\alpha_n\beta_n(\lambda_n)=\beta(\lambda_n).
\end{aligned} \tag{7}$$

Here, the unknown coefficients α_i are the experimental volume fractions to be determined. As an example, this procedure was followed for 3 ml total volume of a two-component mixture consisting of 2 ml of ethanol and 1 ml distilled water irradiated at 1310 nm and 1550 nm. Figures 6 and 7 show the PPE signals for

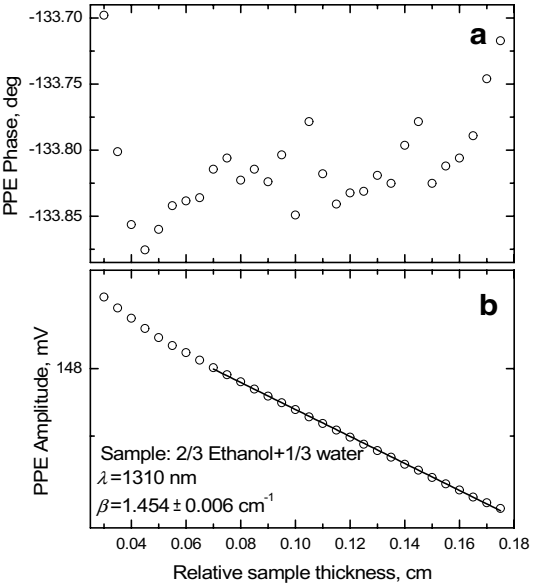

Fig. 6 PPE signal phase (a) and amplitude (b) for a liquid mixture of ethanol and distilled water, volume fraction of 2/3 and 1/3, respectively, at 1310 nm as a function of sample thickness. The solid line in (b) is the linear best fit used for extracting the liquid's optical absorption coefficient at this wavelength

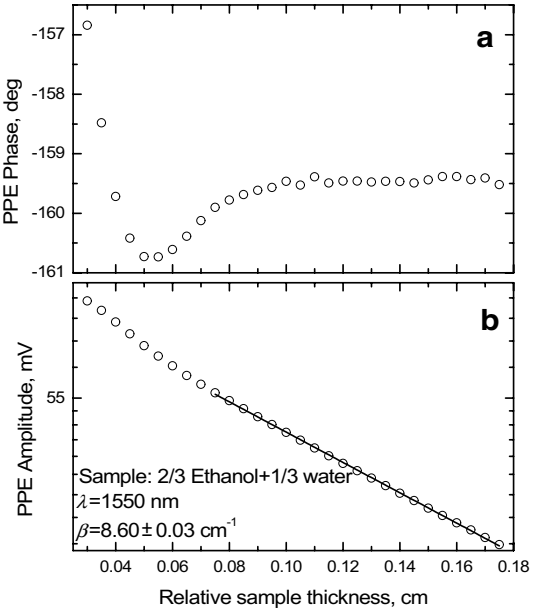

Fig. 7 Photopyroelectric (PPE) signals in phase (a) and amplitude (b), at a wavelength of 1550 nm, as a function of the sample's thickness, for a liquid mixture of ethanol and distilled water, volume fraction of 2/3 and 1/3, respectively. The solid line in (b) is the linear best fit used for extracting the liquid's optical absorption coefficient at this wavelength

the mixture as a function of sample thickness at these two wavelengths. The thus measured corresponding optical absorption coefficients are shown in the same figures. Using values of the two optical absorption coefficients for the pure fluids from Table 1 (distilled water and ethanol at 1310 nm and 1550 nm), the corresponding equation system (7) reduces to two linear equations:

$$\begin{aligned} 2.67\,\alpha_1 + 0.725\,\alpha_2 &= 1.454 \\ 11.62\,\alpha_1 + 6.06\,\alpha_2 &= 8.60' \end{aligned} \tag{8}$$

where α_1 and α_2 are the volumetric fractions for distilled water and ethanol, respectively. The solution of the system Eq. 8 yields the values of $\alpha_1 = 0.332 \pm 0.022$ and $\alpha_2 = 0.782 \pm 0.055$, which compare relatively well with the theoretical values 1/3 and 2/3, respectively (the liquid sample was prepared mixing 2 ml of ethanol and 1 ml of distilled water for a total of 3 ml of mixture). The procedure of estimating the precision on α_i was made here by following the basic rules of error propagation, but other statistical methodologies can be followed [42, 43]. With further, more specific, quantitative studies, this PPE technique could emerge as a "golden standard" technique for liquid molecular property quantification.

6.3 Optical Absorption Coefficient and Quantitative Analysis of Pigments in Liquid Mixtures

An important application of PPE fluid measurements concerns the quantification of pigments in liquid solution. As an example, Fig. 8 shows PPE signals at 690 nm for a set of solutions of copper sulfate of several concentrations (Table 3, column 1) in distilled water. Figure 8a shows the sample thickness range in which the PPE phase remains constant, according to the experimental criterion described above. Figure 8b shows the PPE amplitudes for measuring the corresponding optical absorption coefficients at this wavelength. The continuous lines in this figure are the linear

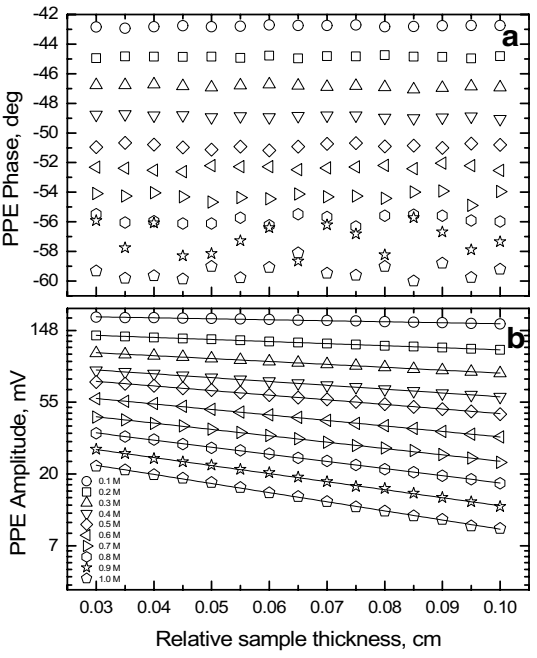

Fig. 8 PPE signal phase (a) and amplitude (b) of aqueous copper sulfate solutions at concentrations described in (b) at 690 nm as a function of sample thickness. The solid line in (b) is the linear best fit used for extracting the liquid's optical absorption coefficient at this wavelength

Table 3 Optical absorption coefficients (β_S) at 690 nm and 785 nm, measured by means of the photopyroelectric technique [29], and the corresponding extracted absorptivities (ε) for water solutions of copper sulfate at different concentrations

Copper sulfate concentration (M)	β_s (690 nm) (cm^{-1})	ε (690 nm) ($cm^{-1}\cdot M^{-1}$)	β_s (785 nm) (cm^{-1})	ε (785 nm) ($cm^{-1}\cdot M^{-1}$)
0.1	1.38 ± 0.04	13.80	2.49 ± 0.03	24.90
0.2	2.88 ± 0.02	14.40	5.65 ± 0.03	28.25
0.3	4.05 ± 0.02	13.50	8.44 ± 0.03	28.13
0.4	5.33 ± 0.03	13.33	11.12 ± 0.03	27.80
0.5	6.42 ± 0.06	12.80	14.07 ± 0.03	28.14
0.6	7.65 ± 0.04	12.84	16.53 ± 0.03	27.55
0.7	8.86 ± 0.08	12.66	19.15 ± 0.18	27.36
0.8	9.96 ± 0.07	12.45	22.92 ± 0.09	28.65
0.9	11.19 ± 0.11	12.43	24.33 ± 0.39	27.03
1.0	12.37 ± 0.12	12.37	27.18 ± 0.27	27.18

best fits for obtaining the optical absorption coefficient for each solution, the corresponding values being summarized in Table 3, column 2. The molar absorptivity of copper sulfate in distilled water at 690 nm was calculated for each of these solutions at known concentration and these values are summarized in Table 3, column 3. This same procedure was followed for copper sulfate samples at a wavelength of 785 nm [29], where this substance absorbs more strongly, the results are summarized in Table 3, columns 4 and 5 (for optical absorption coefficients and absorptivities, respectively). The average of these absorptivities for this last case resulted in $\varepsilon = 27.50 \pm 1.05\ cm^{-1}\cdot M^{-1}$, this means that copper sulfate concentration at any unknown solution can be determined as $c = \beta/27.50$, where β corresponds to the optical absorption coefficient at 785 nm for the unknown sample, measured photopyroelectrically.

The quantification of any other pigment in liquid solution using the PPE technique requires only the measurement of the optical absorption coefficient of the mixture at an appropriate wavelength, provided that the corresponding molar absorptivity is known. If this optical property is unknown, it can be obtained by means of PPE detection by measuring the optical absorption coefficient for a mixture of known concentration (a standard), while making sure that the experimental phase criterion is fulfilled [29, 30].

The phase criterion plays a fundamental role for PPE pigment quantification by simplifying the measurement process of the optical absorption coefficient. Without this criterion the quantification process would be very similar to conventional spectroscopy as it would require the measurement of the optical absorption coefficient for a series of samples at known concentrations to build a calibration curve. This latter procedure was followed for copper sulfate solutions as a matter of comparison with conventional spectroscopy using the optical coefficient values reported in Table 3, column 2. Figure 9 shows the calibration curve exhibiting a linear relation of the optical absorption coefficient as function of the copper

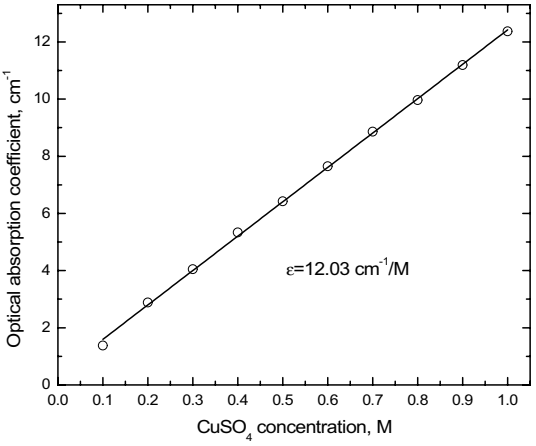

Fig. 9 Optical absorption coefficients of aqueous solutions of copper sulfate at 690 nm as a function of copper sulfate concentration. The solid line is the linear best fit used for extracting the absorptivity of copper sulfate in distilled water

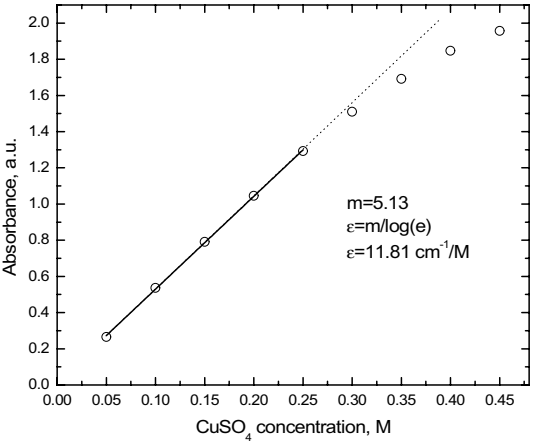

Fig. 10 Absorbance of aqueous solutions of copper sulfate at 690 nm as a function of cupper sulfate concentration. The solid line is the linear best fit used for extracting the absorptivity of copper sulfate in distilled water at this wavelength. Dotted line shows the deviation from the Beer–Lambert model

sulfate concentration, as expected from the Beer–Lambert law. The slope of the linear fit corresponds directly to the absorptivity of copper sulfate in distilled water at 690 nm and was found to be 12.03 $cm^{-1}{\cdot}M^{-1}$. The usual conventional optical spectroscopic procedure for the measurement of this optical property for copper sulfate in water solution is shown in Fig. 10. The absorbances of a set of solutions of copper sulfate in distilled water at 690 nm as a function of fluid mixture concentration in the range of 0.05 M to 0.45 M are shown in this figure. As expected from the Beer–Lambert law, the absorptivity in this case was calculated as the slope of the linear fit to *log(e)* and the result yielded 11.81 $cm^{-1}{\cdot}M^{-1}$ in excellent agreement with the 12.03 $cm^{-1}{\cdot}M^{-1}$ obtained from the PPE technique.

A closer inspection of Figs. 9 and 10 shows the different ranges of pigment concentrations where these two techniques can be applied. Conventional spectroscopy, based on light transmission, is valid at very low concentrations, while

PPES, based on light absorption and non-radiative conversion extends the measurement range to large concentrations.

A novel application of pigment quantification in liquid solution is shown in Fig. 11. In this figure the PPE phase and amplitude for a solution of glucose in distilled water at 1 M is shown as a function of the sample thickness, at a wavelength of 1550 nm. As is shown in the same plot, the optical absorption coefficient for the mixture (obtained as the slope of the best linear fit of the PPE amplitude) at this wavelength was measured to be 12.17 cm^{-1}. The addition rule for optical absorption coefficients, $\beta_{sol} = \beta_{water} + \beta_{gluc}$ applies in this case, where $\beta_{sol} = 12.17\ cm^{-1}$, $\beta_{water} = 11.62\ cm^{-1}$ (Table 1) which yields $\beta_{gluc} = 0.55\ cm^{-1}$. It is concluded that the absorptivity of glucose in distilled water at 1550 nm is $\varepsilon(1550\ nm) = 0.55\ cm^{-1} \cdot M^{-1}$. This result shows the feasibility of glucose measurements in distilled water in the near-infrared region which may lead to establishing minimum glucose concentrations in various applications. This kind of study could also be made at other convenient NIR wavelengths, especially those for which commercial light sources are available.

6.4 Thermal Diffusivity for Quantitative Analysis in Liquid Mixtures

The high precision of thermal diffusivity measurements made feasible with the PPE technique allows the use of this thermophysical property for quantitative analysis. This has been done, for example, in the area of for automotive fuel quality control [37]. A novel application in this area is illustrated here by measuring

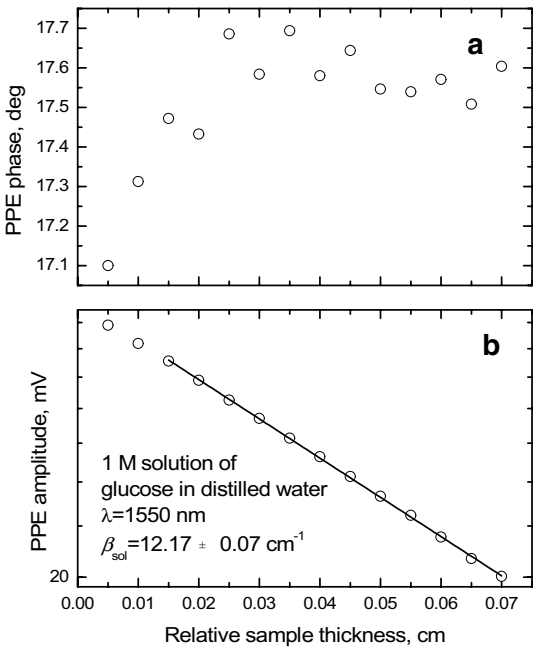

Fig. 11 Photopyroelectric (PPE) signals in phase (a) and amplitude (b), at a wavelength of 1550 nm, as a function of the sample's thickness, for a liquid mixture of glucose in distilled water at 1 M concentration. The solid line in (b) is the linear best fit used for extracting the liquid's optical absorption coefficient at this wavelength

the thermal diffusivity of glucose mixtures in distilled water (Table 4, column 1). The diffusivity of each sample was measured as described in the literature [24, 27]. Figure 12 shows the linear relationship of the PPE amplitude (in semi-log scale) and phase, as functions of sample thickness, as predicted from Eq. 6. Thermal diffusivity values for all samples extracted from the analysis of the PPE amplitude and phase data are summarized in Table 4, columns 2 and 3, respectively. The two values for each sample are close to each other, as expected. Figure 13 shows the behavior of this thermal property as a function of glucose concentration for both, amplitude (circles) and phase (squares). An interesting area for future investigation lies in the relation and physical interpretation of the thermal diffusivity with concentration for this and other carbohydrates (fructose, lactose, etc.)

Table 4 Thermal diffusivities of solutions of glucose in distilled water at different concentrations, measured by means of the photopyroelectric technique [24, 27]

Glucose concentration (M)	α_{Amp} ($cm^2 \cdot s^{-1}$)	α_{Ph} ($cm^2 \cdot s^{-1}$)
0	0.00146	0.00146
0.125	0.00145	0.00145
0.25	0.00144	0.00145
0.375	0.00143	0.00143
0.5	0.00142	0.00142
0.625	0.00139	0.0014
0.75	0.00139	0.00139
0.875	0.00137	0.00138
1.0	0.00136	0.00136
1.125	0.00136	0.00136
1.250	0.00135	0.00135
1.375	0.00134	0.00134
1.5	0.00132	0.00132
1.625	0.00131	0.00132
1.75	0.00130	0.00131
1.875	0.00129	0.00130
2.0	0.00128	0.00129
2.125	0.00128	0.00128
2.25	0.00126	0.00126
2.375	0.00125	0.00126
2.5	0.00124	0.00124

α_{Amp} stands for thermal diffusivity from the analysis of the PPE amplitude and α_{Ph} from the analysis of the PPE phase

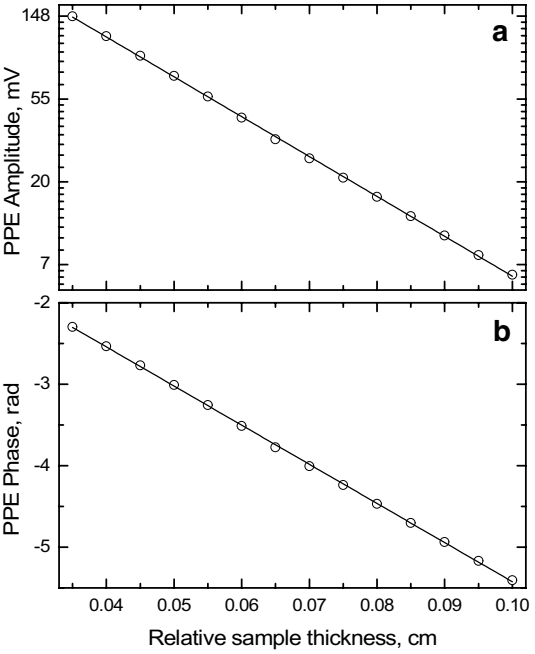

Fig. 12 Photopyroelectric (PPE) signal amplitude (a) and phase (b) for glucose solution in distilled water at 1 M concentration, as a function of sample thickness. The solid lines are the linear best fits used for extracting the liquid's thermal diffusivity in both cases

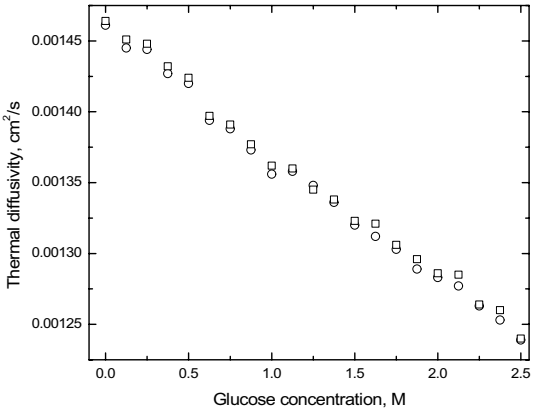

Fig. 13 Thermal diffusivity for water solutions of glucose, from the analysis of the PPE amplitude (circles) and from the analysis of the PPE phase (squares), as a function of the molar concentration

7 Perspectives and Conclusions

In this review, PPE detection principles in fluids and mixtures and state-of-the-art applications were presented. The implementation of pyroelectric sensors for photothermal detection applications has allowed the development of new and more sensitive methods for the study and determination of optical and thermophysical properties of condensed matter. The flexibility of these techniques in selecting control variables such as the wavelength of illumination—radiation, the modulation frequency or the sample thickness as control parameters to be used as inputs

to suitable PPE mathematical models, has allowed the implementation of PPE detection methods for specific optical, molecular and thermophysical measurements in wide classes of materials. Until the mid-1990s most PPE applications were concerned with the optical and thermophysical characterization of solids, using the modulation frequency as variable.

PPE thermal characterization involving modulation frequency as variable has the inconvenience of instrumental (or transfer) function which is difficult or even impossible to model. This inconvenience was overcome with the development of the thermal wave resonator cavity (TWRC) [22]. The PPE theory involving a surface optical absorption (opaque) model allowed the implementation of experimental systems for high-precision measurements of thermal diffusivity of liquids and gases without the need to implement transfer function normalization of signals. The TWRC method has allowed using sample thickness as a control variable in a general optical Beer–Lambert absorption model [28, 29] that has led to the direct measurement of optical absorption coefficients of liquids, opening the field for the development of quantitative PPE analysis in fluids. In comparison with conventional spectroscopy used for the quantitative analysis of fluids, the PPE technique has important qualitative advantages: unlike conventional transmission spectroscopy by means of radiation passing through a fixed sample thickness, PPE involves a tangible experimental criterion (the criterion of the constant phase) for the validity of measuring optical properties. Moreover, no reference sample or calibration curve is required. Furthermore, the optical-to-thermal energy conversion mechanism for PPE signal generation primarily through absorption of radiation in the medium of interest, imparts to PPE a much wider dynamic range than conventional spectroscopy. Due to these advantages and the instrumentation simplicity of PPES, it has been shown that this photothermal modality can perform quantitative analysis for quality control in areas where other optical techniques have important limitations.

As described in this review, PPE measurements of thermal diffusivities and optical absorption coefficients in fluids and mixtures can be important parameters to be used for analytical purposes, both qualitative and quantitative. Some particular issues that remain to be addressed in the further development of PPE detection in fluid systems are:

- The extent to which optical dispersion affects the measurement of optical properties, a key issue in conventional spectroscopy, and related to this, the need to implement more general absorption models.
- The dynamic range of these methodologies.
- A thorough investigation of the utility of using thermal diffusivity and optical absorption coefficient measurements for the quantitative analysis of single- and multi-component liquid mixtures. These are complex issues presenting challenges to conventional spectroscopic techniques.
- Optical absorption coefficients measurements in pure liquids using broadband light sources similar to those used in conventional spectroscopic techniques with considerably simpler instrumentation and signal processing systems.

Acknowledgments A. Mandelis is grateful to the Natural Sciences and Engineering Research Council of Canada (NSERC) for a Discovery grant and to the Canada Research Chairs Program.

References

1. S.G. Porter, A brief guide to pyroelectric detectors. Ferroelectrics **33**, 193 (1981)
2. S.B. Lang, Pyroelectricity: a 2300-year history. Ferroelectrics **7**, 231 (1974)
3. A. Odon, Voltage response of pyroelectric PVDF detector to pulse source of optical radiation. Meas. Sci. Rev. **5**, 55 (2005)
4. U. Zammit, M. Marinelli, F. Mercuri, S. Paoloni, F. Scudieri, Photopyroelectric calorimeter for the simultaneous thermal, optical, and structural characterization of samples over phase transitions. Rev. Sci. Instrum. **82**, 121101 (2011)
5. M. Chirtoc, C. Glorieux, J. Thoen, Thermophysical properties and critical phenomena studied by photopyroelectric (PPE) method, in *Thermal Wave Physics and Related Photothermal Techniques: Basic Principles and Recent Developments*, ed. by E.M. Moraes (Transworld Research Network, Kerala, 2009)
6. H. Coufal, A. Mandelis, Photopyroelectric spectroscopy of semiconductors, in *Photoacoustic and Thermal Wave Phenomena in Semiconductors*, ed. by A. Mandelis (North Holland Publ. Co., Inc., New York, 1987)
7. Ferroelectrics, Special Issue on in *Photopyroelectric Spectroscopy and Detection (PPES)*, ed by A. Mandelis (Guest Editor) (Gordon and Breach Publishers, Amsterdam, 1995)
8. A. Mandelis, Frequency domain photopyroelectric spectroscopy of condensed phases: a new, simple and powerful spectroscopic technique. Chem. Phys. Lett. **108**, 388 (1984)
9. H. Coufal, Photothermal spectroscopy using a pyroelectric thin-film detector. Appl. Phys. Lett. **44**, 59 (1984)
10. A. Mandelis, M.M. Zver, Theory of photopyroelectric spectroscopy of solids. J. Appl. Phys. **57**, 4421 (1985)
11. K. Tanaka, Y. Ichimura, K. Sindoh, Pyroelectric photothermal spectroscopy of thin solid films. J. Appl. Phys. **63**, 1815 (1988)
12. M. Chirtoc, G. Mihâilescu, Theory of the photopyroelectric method for investigation of optical and thermal materials properties. Phys. Rev. B **40**, 9606 (1989)
13. A. Mandelis, J.T. Dodgson, Spectroscopic studies of solids using correlation photoacoustic spectroscopy (CPAS). J. Phys. C: Solid State Phys. **19**, 2329 (1986)
14. J. Caerels, C. Glorieux, J. Thoen, Absolute values of specific heat capacity and thermal conductivity of liquids from different modes of operation of a simple photopyroelectric setup. Rev. Sci. Instrum. **69**, 2452 (1998)
15. A. Mandelis, F. Care, K.K. Chan, L.C.M. Miranda, Photopyroelectric detection of phase transitions in solids. Appl. Phys. A **38**, 117 (1985)
16. M. Marinelli, U. Zammit, F. Mercuri, R. Pizzoferrato, High-resolution simultaneous photothermal measurements of thermal parameters at a phase transition with the photopyroelectric technique. J. Appl. Phys. **72**, 1096 (1992)
17. J. Thoen, C. Glorieux, Photoacoustic and photopyroelectric approach to calorimetric studies. Thermochim. Acta **304/305**, 137 (1993)
18. S.B. Peralta, Z.H. Chen, A. Mandelis, Simultaneous measurement of thermal diffusivity, thermal conductivity and specific heat by impulse response photopyroelectric spectrometry: application to the superconductor $YBa_2Cu_3O_{7-x}$. Appl. Phys. A **52**, 289 (1991)
19. M. Marinelli, F. Murtas, M.G. Mecozzi, U. Zammit, R. Pizzoferrato, F. Scudieri, S. Martellucci, M. Marinelli, Simultaneous determination of specific heat, thermal conductivity and thermal diffusivity at low temperature via the photopyroelectric technique. Appl. Phys. A **51**, 387 (1990)
20. D. Dadarlat, J. Gibkes, D. Bicanic, A. Pasca, Photopyroelectric (PPE) measurement of thermal parameters in food products. J. Food Eng. **30**, 155 (1996)
21. S. Manohar, S. Asokan, Strip inverse-configuration photopyroelectric technique to measure the thermal conductivity of bulk samples. Appl. Phys. Lett. **78**, 469 (2001)
22. J. Shen, A. Mandelis, Thermal-wave resonator cavity. Rev. Sci. Instrum. **66**, 4999 (1995)

23. G. Pan, A. Mandelis, Measurements of the thermodynamic equation of state via the pressure dependence of thermophysical properties of air by a thermal-wave resonant cavity. Rev. Sci. Instrum. **69**, 2918 (1998)
24. J.A. Balderas-López, A. Mandelis, J.A. Garcia, Thermal-wave resonator cavity design and measurements of the thermal diffusivity of liquids. Rev. Sci. Instrum. **71**, 2933 (2000)
25. J.A. Balderas-López, A. Mandelis, Simple, accurate, and precise measurements of thermal diffusivity in liquids using a thermal-wave cavity. Rev. Sci. Instrum. **72**, 2649 (2001)
26. A. Matvienko, A. Mandelis, High-precision and high-resolution measurements of thermal diffusivity and infrared emissivity of water–methanol mixtures using a pyroelectric thermal wave resonator cavity: frequency-scan approach. Int. J. Thermophys. **26**, 837 (2005)
27. J.A. Balderas-López, M.R. Jaime-Fonseca, G. Gálvez-Coyt, A. Muñoz-Diosdado, J. Díaz-Reyes, Generalized photopyroelectric setup for thermal-diffusivity measurements of liquids. Int. J. Thermophys. **36**, 857 (2015)
28. J.A. Balderas-López, Photopyroelectric technique for the measurement of thermal and optical properties of pigments in liquid solution. Rev. Sci. Instrum. **82**, 074905 (2011)
29. J.A. Balderas-López, Generalized 1D photopyroelectric technique for optical and thermal characterization of liquids. Meas. Sci. Technol. **23**, 065501 (2012)
30. J.A. Balderas-López, Y.M. Gómez-Gómez, Photopyroelectric technique for hemoglobin assessment in human blood. Int. J. Thermophys. **36**, 844 (2015)
31. M. Grinberg, A. Mandelis, Photopyroelectric quantum yield spectroscopy and quantum mechanical photo-excitation decay kinetics of the Ti^{3+} ion in Al_2O_3. Phys. Rev. B **49**, 12496 (1994)
32. A. Mandelis, M. Grinberg, Ultrasensitive quadrature photopyroelectric quantum yield spectroscopy of Ti^{3+}:Al_2O_3: evidence for domination of de-excitation mechanism by inter-configurational nonradiative transitions in an unthermalized manifold. Chem. Phys. Lett. **238**, 65 (1995)
33. J. Shen, K. Fjeldsted, J. Vanniasinkam, A. Mandelis, Surface polish characterization of industrial Ti: sapphire laser crystal rods by photopyroelectric scanning imaging. Opt. Mater. **4**, 823 (1995)
34. A. Mandelis, A. da Silva, Quantitative in-situ photopyroelectric spectroscopy of optoelectronic quantum structures. Theory and experiment with Al0.6Ga0.4As/GaAs quantum wells. Ferroelectrics **165**, 1 (1995)
35. J.A. Balderas-López, A. Mandelis, Thermal diffusivity measurements in the photoacoustic open-cell configuration using simple signal normalization techniques. J. Appl. Phys. **90**, 1 (2001)
36. J.A. Balderas-López, M.R. Jaime-Fonseca, G. Gálvez Coyt, A. Muñoz-Diosdado, J.A. Pescador, J. Díaz-Reyes, B.E. Chávez-Sandoval, Photothermal techniques for thermal characterization of linear alcohols. Int. J. Thermophys. **39**, 111 (2018)
37. I.A. Esquef, A.P.L. Siqueira, M.G. da Silva, H. Vargas, L.C.M. Miranda, Photothermal characterization of natural gas automotive fuel. Meas. Sci. Technol. **17**, 1385–1389 (2006)
38. W.S. Pegau, D. Gray, J.R.V. Zaneveld, Absorption and attenuation of visible and near-infrared light in water: dependence on temperature and salinity. Appl. Opt. **36**, 6035 (1997)
39. J.A. Curcio, C.C. Petty, The near infrared absorption spectrum of liquid water. J. Opt. Soc. Am. **41**, 302 (1951)
40. H. Cabrera, A. Marcano, Y. Castellanos, Absorption coefficient of nearly transparent liquids measured using thermal lens spectrometry. Condens. Matter Phys. **9**, 385 (2006)
41. W.M. Irvine, J.B. Pollack, Infrared optical properties of water and ice spheres. Icarus **8**, 324 (1968)
42. J. Mandel, *The Statistical Analysis of Experimental Data* (Dover Publications Inc., New York, 1964)
43. D. González-Gómez, A. Muñoz de la Peña, A. Espinoza Mansilla, A. César Olivieri, Spectrophotometric analysis of mixtures by classical least-squares calibration: an advanced experiment introducing MATLAB. Chem. Educator **8**, 187 (2003)